

Real-time Dynamic Path Planning for Dubins' Nonholonomic Robot

Chao Yong and Eric J. Barth

Department of Mechanical Engineering
Vanderbilt University, Nashville, U.S.A.
[eric.j.barth, chao.yong]@vanderbilt.edu

Abstract – A car-like nonholonomic robot moves in a plane and is subject to an upper bound of curvature for its turning. In this paper, we discuss a novel dynamic path planning algorithm by which the car-like robot could reach any oriented point from another oriented point via the shortest path. The approach features the construction of a pair of accommodation circles describing the left and right turn minimum radius paths of the vehicle. Utilizing this construction, a weak control Lyapunov function is constructed and used to generate a control law. This motion planner provides a real-time state dependent solution with a convergence guarantee.

Index Terms – Motion planning, shortest path, curvature constraints.

I. INTRODUCTION

This paper considers the path planning problem for a nonholonomic robot moving in the plane without obstacles but subject to velocity and turning radius constraints. The goal of this work is to offer a solution to this problem that is continuous and implementable in real-time. Given an initial configuration and a goal configuration, the shortest path planning problem for this type of robot plays a crucial role in motion planning.

Numerous results have been achieved on the shortest path planning problem. Without considering obstacles, pioneer Dubins [1] first addressed this issue: the shortest path consists of at most three sequentially connected either arcs or straight line segments. Reeds and Shepp [2] extended this result to vehicles which can move both forward and backward. Besides these analytic works, Sussmann and Tang [3], and Boissonat et al. [4] proved Dubins' and Reeds and Shepp's work using ideas from control theory. Based on these works, Bui and Soueres [5] then provided a shortest path synthesis for Dubins nonholonomic car. The literature, such as [6][7], is rich in making extensions of shortest path planning without obstacles, to that in the presence of obstacles.

We consider the problem of the shortest path planning for Dubins' nonholonomic robot having a constant linear velocity in the absence of obstacles. Instead of solving this problem in an analytic manner, we try to design a real-time implementable control law by which the robot will be moving along the optimal, or at least a feasible and reasonable suboptimal path, from one configuration to another configuration. As a sub-module, this method can

then be utilized to plan shortest path segments in the presence of obstacles in future work. In order to avoid obstacles, a set of way points would be provided by some existing obstacle detection algorithm. Our algorithm can then operate as a local path planner to follow these way points one by one.

Instead of searching paths for the car's trajectory itself, we propose a novel method of decomposing the car's position and orientation into center points of a pair of **accommodation circles** which define the left and right minimum turning radius paths. Artificial potential field induced forces¹ [8], positive and negative, are generated between matched (e.g. left goal and left initial) or unmatched circle centers (e.g. left goal and right initial). A control Lyapunov function (**CLF**) is then constructed via these potential forces. A control law is designed such that the **CLF** is always non-incrementing. At every instant of time, the control variable is simply computed based on the vehicle's states, without the need for a global map analysis. The work presented here is motivated by the need to formulate a method general enough in its construction to be capable of being extended to solve the considerably more complicated input constrained 3-D nonholonomic path planning problem, especially for UAV applications.

The paper is organized as follows. Section 2 gives definitions and remarks regarding Dubins' shortest path problem. The constructions of attractive potential forces and a Lyapunov stability function are described in section 3. Also in section 3, an additional repulsive potential force is introduced, and consequently the controller is modified in the case where the initial and goal positions are very close. The control law is presented at the end of this section. Finally, section 4 gives some simulation results and discussion.

II. PROBLEM STATEMENT

A. Dubins' Car

A well known model of a simple nonholonomic system, or so called car-like robot, is shown in Figure 1. The robot moves in the 2-dimensional plane in which its position is

¹This “force” is not a true force in the Newtonian sense. In the remainder of the paper, it will be referred to as simply a “force” in this non-strict sense.

determined by the coordinates of the rear wheels (x, y) , while θ is the heading angle with a range of $[-\pi, \pi]$. If the turning radius is lower bounded, as in [11], r is defined as the minimum turning radius. The car's configuration is determined by the triple (x, y, θ) .

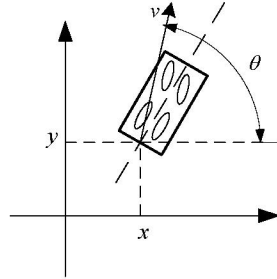


Fig. 1. Model of Dubins' Car

The dynamic model of this nonholonomic system considered in this paper is written in the following form,

$$\begin{cases} \dot{x}(t) = \cos \theta(t) \cdot u_1(t) \\ \dot{y}(t) = \sin \theta(t) \cdot u_1(t) \\ \dot{\theta}(t) = u_2(t) \end{cases} \quad (1)$$

where $u_1(t)$ is the linear velocity and $u_2(t)$ is the angular velocity. For Dubins' car, $u_1(t) \equiv 1$ and $u_2(t) \in (-1, 1)$ for all time t . As a result, the lower bound on the turning radius is $r = 1$. For convenience, we simplify the robot as a particle which has the same properties as those described above.

B. Accommodation Circles

Since the car always turns by the maximum turning rate, it will move on the circle of the lower bounded radius $r = 1$. Bui et al [5] have proven that all shortest path families end with an arc (referred to as "C") or a straight line regressed from such an arc. Inspired by finding the ending circle belonging to this arc, we propose the concept of the accommodation circle.

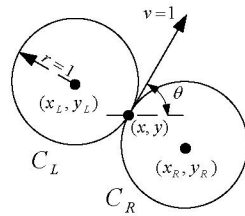


Fig. 2. Decomposing the robot's configuration into left and right accommodation circles.

Definition 2.1: C_L donates the left accommodation circle with center point (x_L, y_L) where subscript L denotes an extreme left-hand turn with minimum turning radius $r = 1$. The robot lies on the circle during a saturated left-hand turn, $u_2 = 1$ in Equation (1), and its linear velocity vector is tangent to the circle. See Figure 2. C_R can be

defined in a symmetric manner. The accommodation circles are defined in the global reference frame, as seen in Fig. 3.

Using two accommodation circles, the robot's configuration is decomposed to the center positions of C_L and C_R , which can be easily obtained from the original configuration (x, y, θ) :

$$\begin{cases} x_L = x - r \sin(\theta) \\ y_L = y + r \cos(\theta) \end{cases}, \begin{cases} x_R = x + r \sin(\theta) \\ y_R = y - r \cos(\theta) \end{cases} \quad (2)$$

The position and orientation of the robot are uniquely determined by the positions of its two accommodation circles, and vice versa. The *accommodation configuration* is thus given by $(x_L, y_L, x_R, y_R, \theta)$ and encodes not only the car's current configuration, as the original triple did, but also encodes the turning rate constraints. In the rest of this paper, L and R denote the center of the car's instant left and right accommodation circle respectively, and L' and R' denote the left and right centers of the goal configuration's accommodation circles respectively.

C. Shortest Paths

For Dubins' car, it has been proven [1][4] that, for any given initial and final configuration, the shortest path consists of a combination of at most three *C* or *S* maneuvers that are continuously connected. Work by Bui et al [5] then proved that the shortest paths exist and are one of the 6 path types of *CCC* and *CSC* families. Within the context of the work presented here, *C* can be represented by L and R which respectively denote turning on the left and right accommodation circle. As denoted in Figure 3, given the initial and final configuration, finding the shortest path for Dubins' car is our basic concern. Previous work mostly

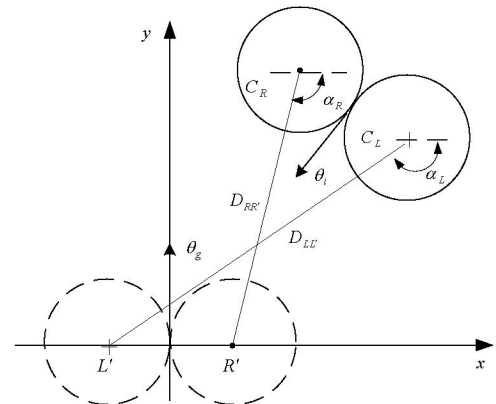


Fig. 3. Shortest path: given initial configuration and goal configuration, the shortest path continuously connects the two configurations.

studied this problem in a manner that would search and analyze the entire remaining path. Here, we approach this problem from a control point of view to arrive at a state-dependent control law and, most importantly, give a general real-time solution to this problem with the motivation of

extending it to the considerably more difficult 3-dimensional case in future work.

To introduce the perspective taken here to formulate the problem, consider the case shown in Figure 3. The initial configuration can be successfully transferred to the goal configuration by moving the center point (x_L, y_L) of C_L and (x_R, y_R) of C_R from their initial positions to $(x_{L'}, y_{L'})$ and $(x_{R'}, y_{R'})$, respectively. Moreover, given that a constant linear velocity is being considered, the best we can achieve is to drive and hold either (x_L, y_L) equal to $(x_{L'}, y_{L'})$ or (x_R, y_R) equal to $(x_{R'}, y_{R'})$ for all time, *but not both*. This characteristic of having to choose one or the other can also been seen in the solution path – it is easy to see that the minimum path length strategy for the configuration shown is to hold the distance $D_{RR'}$ constant or reduce it, without regard to $D_{LL'}$. Had the initial configuration pointed in the opposite direction than shown in Figure 3 (R and L switched), the strategy of holding or reducing $D_{RR'}$ remains the optimal strategy even though $D_{LL'}$ would increase before it decreased. In both cases, $D_{RR'}$ is always less than or equal to $D_{LL'}$ (equal when arriving at the goal configuration). This observation, and similar observations, will form the basis of the potential functions, and ultimately the control Lyapunov function, chosen. Without loss of generality, the final configuration is set to $(0,0,\pi/2)$ in this paper. As a result, L' and R' are always $(-r,0)$ and $(r,0)$ respectively. The robot reaches the goal when $(x_{L'}, y_{L'}) = (-r,0)$ and $(x_R, y_R) = (r,0)$.

III. PROBLEM FORMULATION AND ANALYSIS

As described in the previous section, the car reaches the goal configuration from the initial configuration when its accommodation circles fully overlap the accommodation circles of the goal configuration. In other words, the distances between the center points of corresponding circles are simultaneously zero ($D_{LL'} = 0$ and $D_{RR'} = 0$), and the car reaches the final goal point with the desired orientation. A corollary of this truth is that the distance between L' and R , and between R' and L are ultimately equal to $2r$ in the goal configuration. Motivated by this, we develop a real time controller based on the distances between the centers of the accommodation circles of car's current and goal configurations.

A. Potential Forces

Based on the artificial potential field concept [10], the goal generates an attractive force to pull the car moving toward it. In this paper, the artificial potential forces are generated by the goal's accommodation circles such that car's instant accommodation circles are pulled by their corresponding goal accommodation circles.

Definition 3.1: $D_{LL'}$ is the distance between the car's left accommodation circle center and that of the goal's left accommodation circle center.

$$D_{LL'} = \sqrt{(x_L - x_{L'})^2 + (y_L - y_{L'})^2}$$

Since the final configuration is set as $(0,0,\pi/2)$ without loss of generality,

$$D_{LL'} = \sqrt{(x - r \sin \theta + r)^2 + (y - r \cos \theta)^2} \quad (3)$$

Similarly,

$$D_{RR'} = \sqrt{(x + r \sin \theta - r)^2 + (y + r \cos \theta)^2} \quad (4)$$

Besides the attractive forces between LL' and RR' , repulsive forces between R and L' , L and R' exist under certain condition.

Definition 3.2: Along the goal's orientation direction, the projected distance between R and L' is (see Figure 4),

$$d_{RL'} = y_{L'} - y_R$$

We will define a potential repulsive force to exist only if

$$0 \leq (y_{L'} - y_R) < 2r \quad (5)$$

otherwise it vanishes. Thus the potential distance is

$$D_{RL'} = 2r - d_{RL'} \quad (6)$$

$D_{LR'}$ can be similarly obtained,

$$D_{LR'} = 2r - (y_{R'} - y_L) \quad \text{when } 0 \leq (y_{R'} - y_L) \leq 2r \quad (7)$$

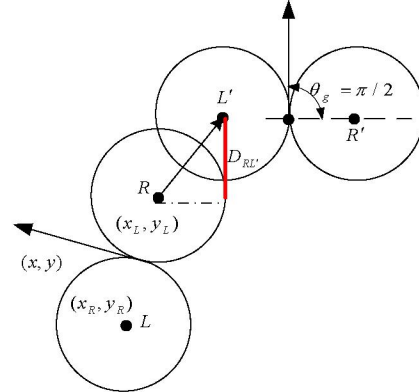


Fig. 4. Repulsive force between right and left accommodation circles

The basic idea behind the potential forces is to make the car avoid some non-optimal paths, which will be discussed in section B2. The potential force pushes the overlapped circles away until they are not overlapped anymore.

B. Control Lyapunov Function

In this section, we build a *weak* control Lyapunov function (**CLF**) for controlling the trajectory of Dubins' car. In our system, the time varying variables that we want to control are the distances defined in the previous section. The **CLF** is thus designed to control them in a proper manner.

Definition 3.3: (see [12]) A control Lyapunov function (**CLF**) for system (1) is a positive-definite, decrescent, radially unbounded function in the time domain.

For our system, the CLF's intrinsic property is to drive all distances to zero. One can easily see those distances become zero when the system reaches the equilibrium point: the goal configuration for our system. We propose the following CLF which satisfies the above requirements, and thus the following candidate function is considered.

$$V(x, y) = \left[(1/x)^n + (1/y)^n \right]^{-1/n} \quad (8)$$

where x, y are positive, and $n \rightarrow \infty$. One can show that $V(t)$ will be significantly closer to the smaller of the two positive independent variables as n is increased. We call this type of function a *vote function* by which the shorter distance is selected. $V(x, y)$ will be decrescent while the shorter element is decrescent. Using this vote function, if the smaller of the two distances defined above is decreased, V itself will be decreased² regardless of whether the larger distance is made to decrease or not. The connection between this property and the characteristics of the problem discussed in section IIC provides a central feature of the proposed method.

B1. Attractive forces

In the case that only attractive forces exist, the $V(x, y)$ can be represented as

$$V_A(t) = \left[(1/D_{LL'})^n + (1/D_{RR'})^n \right]^{-1/n} \quad (9)$$

Bui et al [5] proves that, in this case, the shortest path is one type of CSC family, which means the repulsive force will not exist from this point forward along the optimal path. As a result, the vote function selects the shorter distance of $D_{LL'}$ and $D_{RR'}$. By carefully designing the control law, $V_A(t)$ is always decrescent or semi-decrecent until both distances come to zero, in other word, the car reaches the final configuration. In order to achieve this goal, we have to make $\dot{D}_{LL'} \leq 0$ or $\dot{D}_{RR'} \leq 0$ when one of them is selected.

Differentiating (3) gives

$$\dot{D}_{LL'} = \left(\sqrt{(x - r \sin \theta + r)^2 + y^2} \right)^{-1} (x \cos \theta + y \sin \theta + r \cos \theta) \quad (10)$$

As shown in Figure 3, α_L is the angle of line $L \rightarrow L'$, and

$$\cos \alpha_L = (x_L - x_{L'}) / D_{LL'} \quad (11)$$

Substituting and rearranging,

$$\dot{D}_{LL'} = -(1 + r\dot{\theta}) \cos(\alpha_L - \theta) \quad (12)$$

where $\alpha_L - \theta \in (-\pi, \pi]$ is the angle difference between line $L \rightarrow L'$ and car's heading angle.

Choosing the control signal only from the set of $\{-1, 0, 1\}$ is motivated by the Dubins' result that the optimal path will only use these control signals. Since $\dot{\theta}$ can only be one

²This function is sometimes referred to as a *weak CLF* in that there will exist points in the control formulation where \dot{V} is only made equal to zero and not strictly less than zero, which is not a strict CLF.. However, this function can select the smaller distances and converge both attractive distances to zero.

of the set $\{-1, 0, 1\}$, $(1 + r\dot{\theta})$ is $\{0, 1, 2\}$ respectively, which are all positive. For different ranges of $\alpha_L - \theta$, we have

$$\begin{cases} -1 \leq \cos(\alpha_L - \theta) \leq 0 & \text{when } \begin{cases} \pi/2 < |\alpha_L - \theta| \leq \pi \\ 0 < \cos(\alpha_L - \theta) \leq 1 \end{cases} \\ 0 < \cos(\alpha_L - \theta) \leq 1 & \text{when } |\alpha_L - \theta| \leq \pi/2 \end{cases}$$

Consider each situation.

a) $-\pi/2 < \alpha_L - \theta \leq \pi/2$, where $\dot{D}_{LL'} \leq 0$. In order to move the car in a CSC manner [5], $\alpha_L - \theta = 0$ is preferred. The controller is designed as

$$\dot{\theta} = \begin{cases} 1, & \alpha_L - \theta > 0 \\ 0, & \alpha_L - \theta = 0 \\ -1, & \alpha_L - \theta < 0 \end{cases} \quad (13)$$

b) $\pi/2 < |\alpha_L - \theta| \leq \pi$, where $\dot{D}_{LL'} \geq 0$. The only way to prevent $D_{LL'}$ from increasing is if $1 + r\dot{\theta} = 0$, that is

$$\dot{\theta} = -1, \quad \pi \leq \alpha_L - \theta \leq -\pi/2 \quad \text{or} \quad \pi \geq \alpha_L - \theta > \pi/2 \quad (14)$$

The control law is obtained in the same way in the case that $D_{RR'}$ is selected:

$$\dot{\theta} = \begin{cases} 1, & \alpha_R - \theta > 0 \\ 0, & \alpha_R - \theta = 0 \\ -1, & \alpha_R - \theta < 0 \end{cases} \quad -\pi/2 < \alpha_R - \theta \leq \pi/2 \quad (15)$$

and:

$$\dot{\theta} = 1, \quad \pi \leq \alpha_R - \theta \leq -\pi/2 \quad \text{or} \quad \pi \geq \alpha_R - \theta > \pi/2 \quad (16)$$

With the control laws described above, the controller always tries to first turn the car's heading angle so that $\alpha_L - \theta = 0$, which is a C. Once this is done, the car can move along the line LL' toward a tangent point on the left prime circle, which is an L movement. Finally, if the tangent point is not the goal, it can take a C along the circle to reach the goal. Overall, this path is typically CSC [1] [5], which is the optimal or sub-optimal path. If the first or last step is not needed, the path is a sub family of CSC. More importantly, it can be geometrically proved that the path always exists using this control law when the goal and initial configurations are adequately separated. We will show in simulation that, by selecting the shorter distance, the optimal path is obtained by these control laws.

B2. Repulsive forces

The purpose of the repulsive forces is to eliminate the non-optimal paths generated by the control laws described in last section under certain conditions. Consider the situation shown in Figure 4 for instance. According to the control laws in the last section, if $D_{RR'} < D_{LL'}$ then the path will be RSL and $u + v \geq 2\pi$ which is not the shortest path, where u and v are the angles on the left and right turn arcs [5]. The repulsive forces should then be designed to avoid this solution. The CLF for repulsive force is based on the attractive force version as follows.

$$V_R(t) = e^{-V_A'(t)} \quad (17)$$

$$V'_A(t) = \left[k_L (1/D_{LL})^n + k_R (1/D_{RR})^n \right]^{-1/n} \quad (18)$$

where $k_L = 1$ if (5) is satisfied; otherwise $k_L = 0$. $k_R = 1$ if (7) is satisfied; otherwise $k_R = 0$. When both $k_L = k_R = 1$ $V'_A(t)$ works as same as $V_A(t)$.

Differentiating (17), we have

$$\dot{V}_R(t) = -V_R(t)\dot{V}'_A(t) \quad (19)$$

$\dot{V}'_A(t)$ selects the shorter distances, and gives the proper control input. The repulsive forces invert the control law given in section B1 under conditions $0 \leq (y_{L'} - y_R) < 2r$ or $0 \leq (y_{R'} - y_L) \leq 2r$. For example, in Figure 4, if $D_{RR'} < D_{LL'}$, the corresponding controller is $\dot{\theta} = -1$. The repulsive force makes $\dot{\theta} = 1$ which “pushes” the right accommodation circle away.

B3. Synthesis of attractive and repulsive forces

According to the definitions of potential forces, it can be seen that the attractive forces exist for all time, while the repulsive forces exist only if $0 \leq (y_{L'} - y_R) < 2r$ or $0 \leq (y_{R'} - y_L) \leq 2r$. Again, we can use the vote function idea to select the attractive distances or the repulsive distances that we want to address.

$$V(t) = \left[\left(\frac{1}{V_A(t)} \right)^n + \lambda \left(\frac{1}{V_R(t)} \right)^n \right]^{-1/n} \quad (20)$$

Where n is a natural number with $n \rightarrow \infty$ providing a more accurate solution, λ is zero if both the repulsive forces do not exist and $\lambda = 1$ otherwise. From (9) and (18), it can be seen that $V_A(t)$ and $V_R(t)$ select the same distance, but (17) makes $V_R(t)$ much less than $V_A(t)$ unless $V_A(t)$ is very close to zero. The shortest path and sub-shortest path is then significantly close. In other words, $V_R(t)$ is selected if only it exists, otherwise $V(t) = V_A(t)$.

In this way, if the repulsive forces exist for a given initial configuration, $V(t)$ will select the smaller repulsive force and the corresponding control law takes effect until the repulsive force disappears. After this, $V(t) = V_A(t)$ for the rest of the trajectory.

C. Planning Algorithm

Based on the above discussion, we come to the proposed algorithm which is simple and fast. Given the initial configuration and goal configuration, we first calculate four potential distances. Second, k_1, k_2 are obtained by (5) and (7). These results are then put into (9), (17) and then (20) which gives the distance which we want to decrease. The corresponding control law is then implemented.

Our algorithm only needs to do a simple computation instead of, as many other algorithms do, searching the plane for the shortest path *a priori*. Moreover, the CLF will converge to zero when the car reaches the goal.

IV. SIMULATION EXAMPLES AND DISCUSSION

The proposed planning algorithm has been verified by simulation. Setting the goal configuration to $(0, 0, \pi/2)$, we have tried as many different initial configurations as possible, and the all paths are the shortest. Here we select two initial configurations to discuss our algorithm: the first one does not have repulsive forces (Figure 5) and the second one has both attractive and repulsive forces (Figure 6).

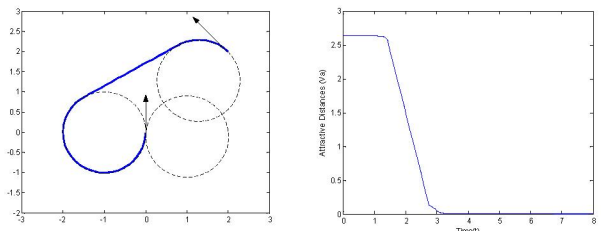


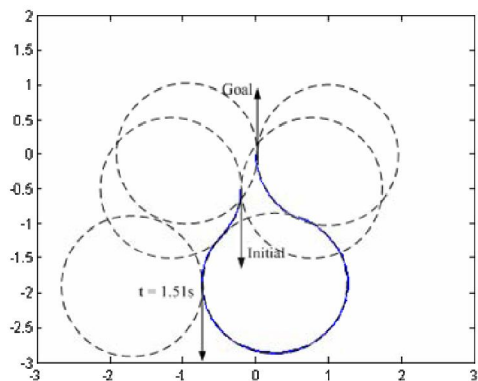
Fig. 5. A case where the car moves with only the attractive forces. a) Trajectory of the car receiving only the attractive forces, b) The CLF for attractive distances

The car moves on the LSL type shortest path in the first example, as shown in Figure 5. Equation (9) gives the shorter distance $D_{LL'}$, and then, according to (13), $\dot{\theta} = -1$ and $D_{LL'}$ consequently remains unchanged until $\alpha_L - \theta = 0$. $D_{LL'}$ then is decreased along the line of $\alpha_L - \theta = 0$ until it is zero. Since $D_{LL'} = 0 \leq D_{RR'}$, it will remain unchanged by moving along the left accommodation circle. $D_{LL'}$ and $D_{RR'}$ then both reach zero leading to the final goal configuration.

It can be seen from Figure 5 b) that The CLF for attractive forces is always semi-positive and semi-descent. One can see that $\alpha_L - \theta = 0$ is a necessary condition which leads the car's instant configuration to the final configuration when only the attractive forces exist. Since the tangent line between two same-side accommodation circles always exist, turning to a proper side will certainly make $\alpha_L - \theta = 0$. In other words, the CLF for attractive forces consequently goes to zero.

As we have seen in the last section, the repulsive distances are always smaller than the attractive distances until they disappear. In the second example shown in Figure 6, the repulsive forces exist before 1.51s. The left accommodation circle of the vehicle will be pushed away first because $D_{LL'}$ is shorter. The right accommodation circle will be pushed away after this and then the repulsive forces disappear. The attractive forces then try to reduce $D_{LL'}$ because it is still shorter than $D_{RR'}$. Actually, if the repulsive force exists, it will be selected because we set it significantly smaller than the attractive force. From b) and c) of Figure 6, we can see that the CLF of the repulsive forces converge first while it makes that of the attractive

forces increase. Once the repulsive forces vanish, the system converges as in the first example.



a) Trajectory of the car receiving both attractive and repulsive forces

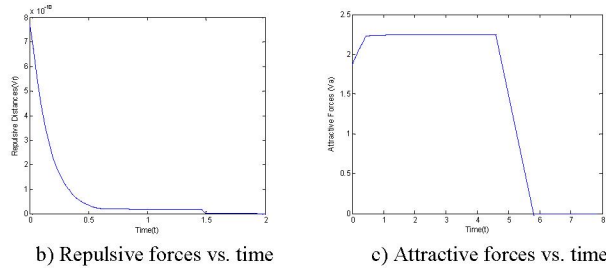


Fig. 6. A case where both attractive and repulsive forces exist (The difficult three-turn solution).

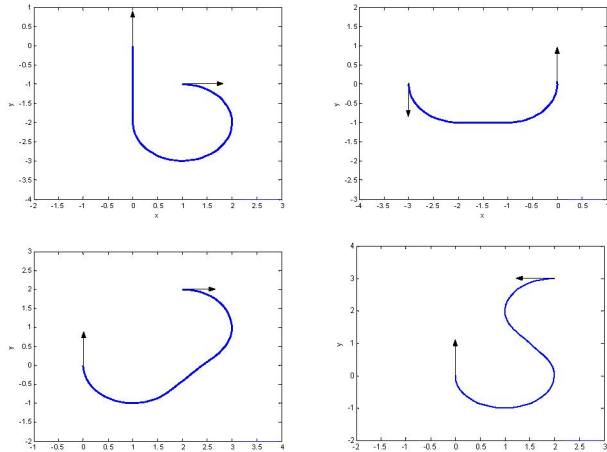


Fig. 7. Other Examples: 1) top left is the RS type shortest path; 2) the top right is the LSL type shortest path; 3) the bottom left is the RSR shortest path; 4) the bottom right is the LSR type shortest path.

Figure 7 shows some other examples which have different types of shortest paths. These results along with the two former examples together are the full families of shortest paths described in [5].

V. CONCLUSION AND FUTURE WORK

In this paper, we have studied the problem of planning trajectories of Dubins' car in the plane. Feasible control

laws are obtained by reducing the distances between corresponding accommodation circles. Some simulation examples have been detailed or briefly shown to verify this new planning method.

Operating as a local planner, this method can be easily adapted to obstacle avoidance based on distance measurement methods [6]. Other applications include following waypoints using this path planning method. This method is also desirable when the goal position is varying or when there are disturbances in the system. This algorithm has a low complexity and is able to be computed in real-time using state-variables. However, the local minima problem might be a concern when our algorithm is applied to avoid obstacles.

Future work is to study the 3-dimensional path planning problem by extending the concepts presented in this work. Unmanned aircraft vehicles would benefit from a computationally fast real-time path planner for agile replanning in the face of changing conditions. Such path planning is much more complicated than 2-D version, but the hope is that similar CLF's using vote functions and generalizations of accommodation circles can be constructed for UAVs and other problems.

REFERENCES

- [1] L.E. Dubins, "On curves of minimal length with a constraint on average curvature and with prescribed initial and terminal positions and tangents," *American Journal of Mathematics*, 79:497-516, 1957.
- [2] J.A. Reeds, R. A. Shepp, "Optimal paths for a car that goes forward and backward," *Pacific Journal of Mathematics*, vol. 145(2), 1990
- [3] H.J. Sussmann, W. Tang, "Shortest paths for the Reeds-Shepp car: a worked out example of the use of geometric techniques in nonlinear optimal control," Report SYCON-91-10, Rutgers Univ., 1991
- [4] J.-D. Boissonnat, A. Cerezo, J. Leblond, "Shortest paths of bounded curvature in the plane," in Proc. IEEE Int. Conf. on Robotics and Automation, 1992
- [5] X. -N. Bui, P. Soueres, J.-D. Boissonnat, and J.-P. Laumond, "Shortest path synthesis for Dubins non-holonomic robots," in Proc. IEEE Int. Conf. on robotics and Automation 1994
- [6] M. Vendittelli, J.P. Laumond, C. Nissoux, "Obstacle distance for car-like robots," Rapport LAAS No99348, IEEE Transactions on Robotics and Automation, Vol.15, NO.4, pp.678-691, August 1999
- [7] L.A. Sanchez, B.J.A. Arenas, R. Zapata, "Optimizing trajectories in non-holonomic motion planning," In 3er Encuentro Internacional de Ciencias de la Computacion. INEGI(2001) 479-488.
- [8] D. Gennery, "Object detection and measurement using stereo vision". In *Proceedings of the 1980 Image Understanding Workshop*, pages 161–167, April 1980.
- [9] L. II. Matthies, "Stereo vision for planetary rovers: stochastic modeling to near real-time implementation," *International Journal of Computer Vision*, 8(1):71- 91, July 1992.
- [10] O. Khatib, "Real-time obstacle avoidance for manipulators and mobile robots," *International Journal of Robotics Research*, 5:90-98, 1986
- [11] J.-D. Boissonnat, A. Cerezo, and J. Leblond, "A note on shortest paths in the plane subject to a constraint on the derivative of the curvature," Research Report 2160, Inst. Nat. de Recherche en Informatique et en Automatique, January 1994.
- [12] E.D. Sontag, "A Lyapunov-like characterization of asymptotic controllability," *SIAM J. Control Optim.*, vol. 21, no. 3, pp. 462-471, May 1983